


Research Article

Effect of Changing Path on Pedestrian Traffic under the Cumulative Effect of Delay Time

Bingling Cen,¹ Yu Xue ,^{1,2} Xue Wang,¹ and Peng Zhang¹

¹Institute of Physical Science and Technology, Guangxi University, Nanning 530004, China

²Key Lab Relativist Astrophys, Nanning 530004, Guangxi, China

Correspondence should be addressed to Yu Xue; yuxuegxu@gxu.edu.cn

Received 21 October 2019; Revised 28 January 2020; Accepted 15 February 2020; Published 24 March 2020

Academic Editor: Yannis Dimakopoulos

Copyright © 2020 Bingling Cen et al. This is an open access article distributed under the Creative Commons Attribution License, which permits unrestricted use, distribution, and reproduction in any medium, provided the original work is properly cited.

In this paper, a lattice hydrodynamic model of two-dimensional bidirectional pedestrian traffic is proposed with consideration of altering path under the cumulative effect of delay time. The stability condition is acquired by linear analysis, and the mKdV equation to describe congestion evolution is derived by reductive perturbation technique. According to the result from the stability analysis, the stability region of pedestrian flow can be divided into stable region, unstable region, and metastable region. On the basis of stable condition, the unstable region is narrowed with the increase of delay time t_d and the path changing rate γ . It indicates that changing path can effectively improve the stability of the pedestrian flow under the cumulative effect of delay time t_d . For numerical simulation and analysis of density wave, it is found that the increase of path changing rate γ and the cumulative effect of delay time t_d are conducive to alleviate pedestrian congestion.

1. Introduction

With the increase of urbanization process, the study of city traffic system has become the hot spot which the scientific and social pays attention. As an important part of the city traffic system, pedestrian transportation system brings great convenience for people to travel. But in recent years, the pedestrian stampedes events happened frequently, which has brought serious disasters to the society and brought pain to the victims' families. On December 31, 2014, 36 people were killed and 49 injured in a stampede at Chen Yi Square on the Bund in Shanghai [1]. Saudi authorities issue the Hajj stampede in Mecca on September 26, 2015, have killed 769 people, and wounded 934 others who are from different countries [2]. The stampede caused 22 deaths and 27 injured in Mumbai, India, on September 29, 2017 [3]. How to keep evacuate people safely and effectively in limited space has attracted major concern.

In order to better solve the problem of pedestrian traffic congestion, researchers have made a lot of efforts. From about 1980 onwards, research on pedestrian traffic was often divided into two branches: pedestrian simulation and

pedestrian model. Pedestrian simulation focuses on reproducing the natural behavior of pedestrian flow. And with the development of computer graphics, virtual pedestrians can be realized.

There are many similar behaviors and different characteristics between the vehicular traffic and the pedestrian traffic. First of all, on the macro level, pedestrian traffic presents the same flow characteristics as vehicle traffic. Similarly, the average velocity and flux can be introduced to describe flow characteristics. However, pedestrian traffic composed of the different individuals shows stochastic properties and multidirection movement due to fewer constraints. Thus, pedestrian traffic is more complex and flexible than vehicular traffic. Henderson firstly put forward the macroscopic model of pedestrian flow in 1971 by applying gas dynamics model and fluid dynamics model to the crowd experience data. He argued that the crowd's behavior is similar to gas under the freely moving phase with low density and similar to fluids under congested phase with high density. However, the energy conservation in the interaction of pedestrians cannot be satisfied in case of pedestrian conflict [4]. In 1992, Helbing proposed a better fluid

dynamics model on the basis of Henderson's model by taking into account the intention, the desired velocity, and interaction between pedestrians [5]. Hughes' model of crowd gives the following three assumptions: (1) pedestrian velocity is only determined by the pedestrian density; (2) pedestrian has about the destination of the common sense; and (3) pedestrians seek the shortest travel time [6]. Existing pedestrian models mainly include cellular automata model, lattice gas model, agent-based model, social force model, and hydrodynamic model [4, 7–20]. Helbing and Molnár presented the social force model to describe pedestrian dynamics in 1995 and assumed that the interaction between pedestrians and pedestrians and between pedestrians and environment is expressed by social forces [21]. But it will cause unexpected effects when the superposition principle of force is satisfied under high density. Cellular automata model (CA model) of pedestrian traffic flow is a micromodel which discretizes time and space. Introducing the cellular automata model of traffic flow into pedestrian flow, it is necessary to refine the discrete space. Each pedestrian to occupy the multiple cells selects the moving direction and speed according to the simple rules [22]. At present, these models have been used for pedestrian facility design, calculation of channel capacity, and emergency evacuation. And many characteristics of pedestrian traffic can be extensively applied to many occasions such as bidirection pedestrian, fire evacuation, aircraft evacuation, T-shaped intersection, bottleneck road section, and slope evacuation [23–27].

Comparing with micro-CA model, the macroscopic model is suitable to real-time online simulate pedestrian flow and carry out prediction due to the neglect of pedestrian movement details resulting in rapid calculation. The first microlattice hydrodynamic model was put forward by Nagatani in 1998. He simplified Kerner and Konhäuser's high-order continuous model and referenced to the idea of the car-following model obtained by flow dynamics equation and conservation equation [28]. And for simulating more actual status of traffic flow, Nagatani proposed a two-lane traffic model to consider the problem of vehicle lane change in 1999 [29]. When the motion of a crowd is seen as fluid flow at a macrolevel, the lattice dynamic equations describing the flow can be applied to pedestrian traffic. Based on Nagatani's lattice hydrodynamic model, Tian et al. extended the two-lane lattice hydrodynamic model of traffic flow to the two-dimensional lattice hydrodynamic model considering path change in bidirectional pedestrian traffic flow and studied the impact of path changing rate on the stability of pedestrian traffic flow through discussing the value of critical point a_c [30, 31]. Kuang et al. presented a new lattice hydrodynamic model for two-way pedestrian flow considering pedestrian visual field effect. The phase transitions between the freely moving phase, the coexistence phase, and the jamming phase below which the critical point a_c has been found [32]. Zhou et al. studied the effect of memory effect on pedestrian flow and assumed pedestrians may walk by his memory when it is difficult for pedestrians to accurately capture the position [33]. Li et al. extended the original hydrodynamic model of traffic flow to single row

pedestrian movement with medium and high density and considered asymmetric interaction [34]. Yu et al. solve the general solution of the mKdV (modified Korteweg–de Vries) equation [35]. In 2015, Redhu and Gupta present a new lattice hydrodynamic model based on delayed feedback control considering the flow difference effect [36]. In 2016, Redhu and Gupta propose a multiphase lattice hydrodynamic model by considering the forward looking effect and discuss the impact of forward leading lattices on multiphase traffic dynamics [37]. Peng et al. consider the lateral effects and extended the lattice hydrodynamic model to the non-lane-based lattice hydrodynamic model [38]. Wang et al. study the impact of the multiple density difference effect on the stability of traffic [39].

Until now, the lattice hydrodynamic model of pedestrian flow with consideration of path change has been little developed. Also, the cumulative effect of delay time is important to adjust current pedestrian flow reaching the optimal status. The movement of pedestrians will be affected by the transverse effect and the longitudinal effect between them. Assumed that if there is more space to allocate pedestrian in the transverse direction based on the optimal effect and comfort level, one can select to continue along the way forward or also select to change path with a faster rate. In the longitudinal direction, Tian et al. have studied that the current grid point flow is adjusted by the optimized flow of the grid point ahead. The pedestrian flow reaches the optimal flow within the delay time t_d , while the downstream optimal flow can continuously adjust the current flow under the cumulative action of the delay time. Considering both the transverse and longitudinal effects of pedestrian traffic, the analysis of pedestrian traffic evolution characteristics will be more real.

In this paper, a lattice hydrodynamic model of change path pedestrian traffic under the cumulative action of delay time is presented in Section 2. Section 3 carries out the linear stability analysis to obtain the stability condition. In Section 4, the mKdV equation of congestion evolution is derived by applying perturbation theory to perform nonlinear analysis. Section 5 executes the numerical simulation to analyze the evolution of the density wave to discuss the impact of the cumulative effect of delay time. Finally, the main conclusion is simply summarized.

2. Models

In 1999, Nagatani extended the one-lane lattice model to two-lane traffic lattice model and assumed the changing lane happens when the density $\rho_{2,j-1}(t)$ at site $j-1$ on the second lane is greater than the density $\rho_{1,j}(t)$ at site j on the first lane, and the changing lane rate is $\gamma|\rho_0^2 V(\rho_0)|(\rho_{2,j-1}(t) - \rho_{1,j}(t))$, where $\rho_{2,j}(t)$ and $\rho_{1,j}(t)$, respectively, denote the local density at site j on the second lane and the local density at site j on the first lane. The changing path frequency is denoted as γ , which reflects the strength of the changing path. The total average density is ρ_0 and the corresponding first derivative is $V(\rho_0) = dV(\rho)/d\rho|_{\rho=\rho_0}$. The velocity $V(\rho_0)$ is called the optimal velocity function of the density ρ_0 , which is defined as follows [28]:

$$V(\rho) = \frac{v_{\max}}{2} \left[\tanh\left(\frac{2}{\rho_0} - \frac{\rho}{\rho_0^2} - \frac{1}{\rho_c}\right) + \tanh\left(\frac{1}{\rho_c}\right) \right], \quad (1)$$

where v_{\max} denotes the maximal velocity of traffic flow and ρ_c represents the critical density which is the inflection point of the function of optimization velocity $V(\rho)$. Similarly, if the density at site j on the first lane is greater than that at site $j+1$ on the second lane, the changing lane rate from the first lane to the second lane is $\gamma|\rho_0^2 V'(\rho_0)|(\rho_{1,j}(t) - \rho_{2,j+1}(t))$.

The conservation equation of one-dimensional lattice hydrodynamic model is expressed as follows:

$$\partial_t \rho_j + \rho_0(\rho_j v_j - \rho_{j-1} v_{j-1}) = \gamma|\rho_0^2 V'(\rho_0)|(\rho_{j+1} - 2\rho_j + \rho_{j-1}), \quad (2)$$

where $\rho_j = (1/2)(\rho_{1,j} + \rho_{2,j})$, $\rho_j v_j = (1/2)(\rho_{1,j} v_{1,j} + \rho_{2,j} v_{2,j})$.

We will extend equation (2) to two-dimensional pedestrian flow with consideration of pedestrian changing path. Pedestrians usually change travelling path along the transverse direction in Public Square and so on. As shown in Figure 1, four-way pedestrian traffic is considered: eastbound, westbound, northbound, and southbound pedestrian. Assumed the fraction of pedestrians moving along each direction is different. The ratio of eastbound and westbound pedestrians to total pedestrians is C , in which the ratio of westbound pedestrians to eastbound is C_1 and the westbound pedestrians correspond to $(1 - C_1)$. The ratio of northbound and southbound pedestrians to total pedestrians is $(1 - C)$. The ratio of southbound pedestrians to southbound is C_2 and the northbound pedestrian is $(1 - C_2)$. The eastbound, westbound, northbound, and southbound pedestrian local densities at site (j, m) at time t are represented by $\rho_{x+}(j, m, t)$, $\rho_{x-}(j, m, t)$, $\rho_{y+}(j, m, t)$ and $\rho_{y-}(j, m, t)$, respectively. The average density can be obtained as follows:

$$\begin{aligned} \rho_{0x+}(j, m, t) &= CC_1 \rho_0, \\ \rho_{0x-}(j, m, t) &= C(1 - C_1) \rho_0, \\ \rho_{0y+}(j, m, t) &= (1 - C)C_2 \rho_0, \\ \rho_{0y-}(j, m, t) &= (1 - C)(1 - C_2) \rho_0. \end{aligned} \quad (3)$$

The conservation equation of the two-dimensional bidirectional pedestrian traffic flow can be written as follows:

$$\begin{aligned} \partial_t \rho(j, m, t) &+ cc_1 \rho_0 [q_{x+}(j, m, t) - q_{x+}(j-1, m, t)] \\ &+ c(1 - c_1) \rho_0 [q_{x-}(j, m, t) - q_{x-}(j+1, m, t)] \\ &+ (1 - c)c_2 \rho_0 [q_{y+}(j, m, t) - q_{y+}(j, m-1, t)] \\ &+ (1 - c)(1 - c_2) \rho_0 [q_{y-}(j, m, t) - q_{y-}(j, m+1, t)] \\ &= \gamma|\rho_0^2 V'(\rho_0)| [\rho(j-1, m-1, t) + \rho(j+1, m-1, t) \\ &+ \rho(j-1, m+1, t) + \rho(j+1, m+1, t) - 4\rho(j, m, t)], \end{aligned} \quad (4)$$

where $\partial_t = \partial/\partial t$. The eastbound, westbound, northbound, and southbound pedestrian flows are denoted as $q_{x+}(j, m, t)$, $q_{x-}(j, m, t)$, $q_{y+}(j, m, t)$ and $q_{y-}(j, m, t)$, respectively.

To simulate more realistic pedestrian traffic conditions with consideration of the impact of downstream pedestrian flow on current pedestrians, the evolution equation of one-dimensional pedestrian traffic flow is obtained as follows:

$$\begin{aligned} \partial_t (q(j, t)) &= a \rho_0 V(\rho(j+1, t)) - a \rho(j, t) v(j, t) \\ &+ a \lambda \int_{t-t_d}^t (\rho_0 V(\rho(j+1, s)) - \rho(j, s) v(j, s)) ds, \end{aligned} \quad (5)$$

where q_j is the pedestrian flow at site j at time t and a is the sensitivity coefficient of pedestrian flow (the inverse of the response time τ). In effect, the response time is a relaxation time when the pedestrian flow reaches a steady state from a nonequilibrium state, which corresponds to the time interval in response to a stimulus. λ denotes the strength coefficient, and the integral term represents the cumulative effect of downstream optimization flow and current pedestrian flow differences within delay time t_d . The delay time t_d is the time pedestrian needs to make decisions about what to travel next and its value is larger than the response time. We employ the following trapezoidal integral formula to approximately estimate integral in equation (5) and extend to four-way pedestrian flow:

$$\begin{aligned} &\int_{t-t_d}^t (\rho_0 V(\rho(j+1, s)) - \rho(j, s) v(j, s)) ds \\ &= \frac{t_d}{2} [\rho_0 V(\rho(j+1, t)) - \rho(j, t) v(j, t) \\ &+ \rho_0 V(\rho(j+1, t-t_d)) - \rho(j, t-t_d) v(j, t-t_d)]. \end{aligned} \quad (6)$$

The evolution equation of four-way pedestrians flow can be written as follows:

$$\begin{aligned}
\partial_t q_{x^+}(j, m, t) &= acc_1 \rho_0 V(\rho(j+1, m, t)) - a q_{x^+}(j, m, t) + \frac{1}{2} a \lambda t_d [cc_1 \rho_0 V(\rho(j+1, m, t)) + cc_1 \rho_0 V(\rho(j+1, m, t-t_d))] \\
&\quad - q_{x^+}(j, m, t) - q_{x^+}(j, m, t-t_d) \\
\partial_t q_{x^-}(j, m, t) &= ac(1-c_1) \rho_0 V(\rho(j-1, m, t)) - a q_{x^-}(j, m, t) + \frac{1}{2} a \lambda t_d [c(1-c_1) \rho_0 V(\rho(j-1, m, t)) \\
&\quad + c(1-c_1) \rho_0 V(\rho(j-1, m, t-t_d))] - q_{x^-}(j, m, t) - q_{x^-}(j, m, t-t_d) \\
\partial_t q_{y^+}(j, m, t) &= a(1-c)c_2 \rho_0 V(\rho(j, m+1, t)) - a q_{y^+}(j, m, t) + \frac{1}{2} a \lambda t_d [(1-c)c_2 \rho_0 V(\rho(j, m+1, t)) \\
&\quad + (1-c)c_2 \rho_0 V(\rho(j, m+1, t-t_d))] - q_{y^+}(j, m, t) - q_{y^+}(j, m, t-t_d) \\
\partial_t q_{y^-}(j, m, t) &= a(1-c)(1-c_2) \rho_0 V(\rho(j, m-1, t)) - a q_{y^-}(j, m, t) + \frac{1}{2} a \lambda t_d [(1-c)(1-c_2) \rho_0 V(\rho(j, m-1, t)) \\
&\quad + (1-c)(1-c_2) \rho_0 V(\rho(j, m-1, t-t_d))] - q_{y^-}(j, m, t) - q_{y^-}(j, m, t-t_d).
\end{aligned} \tag{7}$$

By eliminating velocity in equations (4) and (7), the density evolution equation of four-way pedestrian flow is derived as follows:

$$\begin{aligned}
&\partial_t^2 \rho(j, m, t) + a \partial_t \rho(j, m, t) + a(cc_1)^2 \rho_0^2 [V(\rho(j+1, m, t)) - V(\rho(j, m, t))] \\
&\quad + ac^2(1-c_1)^2 \rho_0^2 [V(\rho(j-1, m, t)) - V(\rho(j, m, t))] + a(1-c)^2 c_2^2 \rho_0^2 [V(\rho(j, m+1, t)) - V(\rho(j, m, t))] \\
&\quad + a(1-c)^2(1-c_2)^2 \rho_0^2 [V(\rho(j, m-1, t)) - V(\rho(j, m, t))] \\
&\quad - a\gamma |\rho_0^2 V'(\rho_0)| [\rho(j-1, m-1, t) + \rho(j+1, m-1, t) + \rho(j-1, m+1, t) + \rho(j+1, m+1, t) - 4\rho(j, m, t)] \\
&\quad + \frac{1}{2} a \lambda t_d (cc_1)^2 \rho_0^2 [V(\rho(j+1, m, t)) + V(\rho(j+1, m, t-t_d)) - V(\rho(j, m, t)) - V(\rho(j, m, t-t_d))] \\
&\quad + \frac{1}{2} a \lambda t_d c^2 (1-c_1)^2 \rho_0^2 [V(\rho(j-1, m, t)) + V(\rho(j-1, m, t-t_d)) - V(\rho(j, m, t)) - V(\rho(j, m, t-t_d))] \\
&\quad + \frac{1}{2} a \lambda t_d (1-c)^2 c_2^2 \rho_0^2 [V(\rho(j, m+1, t)) + V(\rho(j, m+1, t-t_d)) - V(\rho(j, m, t)) - V(\rho(j, m, t-t_d))] \\
&\quad + \frac{1}{2} a \lambda t_d (1-c)^2 (1-c_2)^2 \rho_0^2 [V(\rho(j, m-1, t)) + V(\rho(j, m-1, t-t_d)) - V(\rho(j, m, t)) - V(\rho(j, m, t-t_d))] \\
&\quad + \frac{1}{2} a \lambda t_d \left[\partial_t \rho(j, m, t) - \gamma |\rho_0^2 V'(\rho_0)| [\rho(j-1, m-1, t) + \rho(j+1, m-1, t) + \rho(j-1, m+1, t) \right. \\
&\quad \left. + \rho(j+1, m+1, t) - 4\rho(j, m, t)] \right] \\
&\quad + \frac{1}{2} a \lambda t_d \left[\partial_t \rho(j, m, t-t_d) - \gamma |\rho_0^2 V'(\rho_0)| [\rho(j-1, m-1, t-t_d) + \rho(j+1, m-1, t-t_d) + \rho(j+1, m+1, t-t_d) \right. \\
&\quad \left. + \rho(j+1, m+1, t-t_d) - 4\rho(j, m, t-t_d)] \right] \\
&= \gamma |\rho_0^2 V'(\rho_0)| [\partial_t \rho(j-1, m-1, t) + \partial_t \rho(j+1, m-1, t) + \partial_t \rho(j-1, m+1, t) + \partial_t \rho(j+1, m+1, t) - 4\partial_t \rho(j, m, t)].
\end{aligned} \tag{8}$$

3. Linear Stability Analysis

To obtain the stability condition of equation (8), the linear stability analysis of the lattice hydrodynamic model is performed as follows. At first, we consider the uniform pedestrian flow which has constant density ρ_0 and

optimization velocity $V(\rho_0)$. The solution of the uniform steady state is obtained as $\rho_{j,m}(t) = \rho_0$, $v_{j,m}(t) = V(\rho_0)$. Under disturbance $y(j, m, t)$, the density of pedestrian flow is expressed as $\rho_{j,m}(t) = \rho_0 + y_{j,m}(t)$. Substituting it into equation (8), the linearized equation is derived as follows:

$$\begin{aligned}
& \partial_t^2 y(j, m, t) + a \partial_t y(j, m, t) + a(cc_1)^2 \rho_0^2 V'(\rho_0) [y(j+1, m, t) - y(j, m, t)] \\
& + ac^2(1-c_1)^2 \rho_0^2 V'(\rho_0) [y(j-1, m, t) - y(j, m, t)] + a(1-c)^2 c_2^2 \rho_0^2 V'(\rho_0) (y(j, m+1, t) - y(j, m, t)) \\
& + a(1-c)^2(1-c_2)^2 \rho_0^2 V'(\rho_0) (y(j, m-1, t) - y(j, m, t)) \\
& - a\gamma \rho_0^2 V'(\rho_0) [y(j-1, m-1, t) + y(j+1, m-1, t) + y(j-1, m+1, t) + y(j+1, m+1, t) - 4y(j, m, t)] \\
& + \frac{1}{2} a \lambda t_d (cc_1)^2 \rho_0^2 V'(\rho_0) [y(j+1, m, t) + y(j+1, m, t-t_d) - y(j, m, t) - y(j, m, t-t_d)] \\
& + \frac{1}{2} a \lambda t_d c^2 (1-c_1)^2 \rho_0^2 V'(\rho_0) [y(j-1, m, t) + y(j-1, m, t-t_d) - y(j, m, t) - y(j, m, t-t_d)] \\
& + \frac{1}{2} a \lambda t_d (1-c)^2 c_2^2 \rho_0^2 V'(\rho_0) [y(j, m+1, t) + y(j, m+1, t-t_d) - y(j, m, t) - y(j, m, t-t_d)] \\
& + \frac{1}{2} a \lambda t_d (1-c)^2 (1-c_2)^2 \rho_0^2 V'(\rho_0) [y(j, m-1, t) + y(j, m-1, t-t_d) - y(j, m, t) - y(j, m, t-t_d)] \\
& + \frac{1}{2} a \lambda t_d \left[\partial_t y(j, m, t) - \gamma \rho_0^2 V'(\rho_0) [y(j-1, m-1, t) + y(j+1, m-1, t) + y(j-1, m+1, t) \right. \\
& \left. + y(j+1, m+1, t) - 4y(j, m, t)] \right] + \frac{1}{2} a \lambda t_d \left[\partial_t y_{x+}(j, m, t-t_d) - \gamma \rho_0^2 V'(\rho_0) [y(j-1, m-1, t-t_d) \right. \\
& \left. + y(j+1, m-1, t-t_d) + y(j-1, m+1, t-t_d) + y(j+1, m+1, t-t_d) - 4y(j, m, t-t_d)] \right] \\
& = \gamma \rho_0^2 V'(\rho_0) \left[\partial_t y(j-1, m-1, t) + \partial_t y(j+1, m-1, t) + \partial_t y(j-1, m+1, t) + \partial_t y(j+1, m+1, t) - 4\partial_t y(j, m, t) \right].
\end{aligned} \tag{9}$$

Letting the disturbance $y(j, m, t)$ be expressed as a Fourier series $y(j, m, t) \sim \exp(ik(j+m) + zt)$ and

substituting it into equation (9), we can gain the following equation:

$$\begin{aligned}
& z^2 + az + a(cc_1)^2 \rho_0^2 V'(\rho_0) [e^{ik} - 1] + ac^2(1-c_1)^2 \rho_0^2 V'(\rho_0) [e^{-ik} - 1] + a(1-c)^2 c_2^2 \rho_0^2 V'(\rho_0) [e^{ik} - 1] \\
& + a(1-c)^2(1-c_2)^2 \rho_0^2 V'(\rho_0) [e^{-ik} - 1] - a\gamma \rho_0^2 V'(\rho_0) [e^{-2ik} + 1 + 1 + e^{2ik} - 4] \\
& + \frac{1}{2} a \lambda t_d (cc_1)^2 \rho_0^2 V'(\rho_0) [e^{ik} + e^{ik-zt_d} - 1 - e^{-zt_d}] + \frac{1}{2} a \lambda t_d c^2 (1-c_1)^2 \rho_0^2 V'(\rho_0) [e^{-ik} + e^{-ik-zt_d} - 1 - e^{-zt_d}] \\
& + \frac{1}{2} a \lambda t_d (1-c)^2 c_2^2 \rho_0^2 V'(\rho_0) [e^{ik} + e^{ik-zt_d} - 1 - e^{-zt_d}] + \frac{1}{2} a \lambda t_d (1-c)^2 (1-c_2)^2 \rho_0^2 V'(\rho_0) [e^{-ik} + e^{-ik-zt_d} - 1 - e^{-zt_d}] \\
& + \frac{1}{2} a \lambda t_d \left[z - \gamma \rho_0^2 V'(\rho_0) [e^{-2ik} + e^{2ik} - 2] \right] + \frac{1}{2} a \lambda t_d \left[ze^{-zt_d} - \gamma \rho_0^2 V'(\rho_0) [e^{-2ik-zt_d} + e^{-zt_d} + e^{-zt_d} + e^{2ik-zt_d} - 4e^{-zt_d}] \right] \\
& = \gamma \rho_0^2 V'(\rho_0) \left[ze^{-2ik} + z + z + ze^{2ik} - 4z \right].
\end{aligned} \tag{10}$$

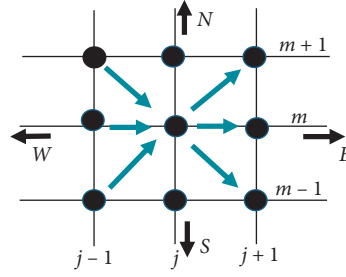


FIGURE 1: The schematic of the pedestrian change of path. The circles denote a pedestrian in the lattice.

By performing Taylor expansion $z = z_1 ik + z_2 (ik)^2 + \dots$ for z and keeping the first- and second-order terms of (ik) , we can abstract the following equation from equation (10):

$$z_1 = -g\rho_0^2 V'(\rho_0)$$

$$z_2 = \frac{-2(g\rho_0^2 V'(\rho_0))^2 - af\rho_0^2 V'(\rho_0)(1 + \lambda t_d) + 8a\gamma|\rho_0^2 V'(\rho_0)|(1 + \lambda t_d)}{2a(1 + \lambda t_d)}, \quad (11)$$

where $g = (cc_1)^2 + ((1-c)c_2)^2 - ((1-c)(1-c_2))^2 - (c(1-c_1))^2$, $f = (cc_1)^2 + ((1-c)c_2)^2 + ((1-c)(1-c_2))^2 + (c(1-c_1))^2$. The uniform steady-state flow becomes unstable pedestrian flow for long-wavelength modes in the condition if z_2 is a negative value. When z_2 is a positive value, the state of the steady flow maintains. The neutral stability condition can be obtained as follows:

$$a > -\frac{2g^2\rho_0^2 V'(\rho_0)}{f(1 + \lambda t_d) + 8\gamma(1 + \lambda t_d)}. \quad (12a)$$

When $\gamma=0.0$, the following stability condition is obtained:

$$a > \frac{-2g^2\rho_0^2 V'(\rho_0)}{f + \lambda t_d f}. \quad (12b)$$

The stability condition is identical with the solution of the lattice hydrodynamic model of bidirectional pedestrian traffic presented by Cen et al. [40]. By comparing the stability condition, we discovered that the critical value of the sensitivity coefficient without changing path frequency is larger than the critical value of the sensitivity coefficient considering changing path frequency. It shows the importance of considering changing lane to alleviate traffic congestion. Moreover, if the cumulative effect of delay time t_d is not taken into account, the stability condition equation (12a) become as follows:

$$a > -\frac{2g^2\rho_0^2 V'(\rho_0)}{f + 8\gamma}. \quad (12c)$$

It is the same as the research results in [31]. Thus, it indicates the cumulative effect of delay time t_d is conducive to suppress traffic jamming.

4. Nonlinear Analysis

Using the reductive perturbation technique to equation (8), we carry out nonlinear analysis by considering long-wave patterns in pedestrian flow on coarse-grained scales. In order to describe the long-wave modes, the slowly varying behavior of long wavelengths near the critical point (ρ_c, a_c) is studied. Introducing a small parameter ε ($0 < \varepsilon \ll 1$), we defined the slow space variables X and slow time variable T :

$$X = \varepsilon(j + m + bt),$$

$$T = \varepsilon^3 t, \quad (13)$$

where b is an undetermined constant. The instantaneous density is obtained as follows:

$$\rho(j, m, t) = \rho_c + \varepsilon R(X, T), \quad (14)$$

using equations (13) and (14) and expanding each term of equation (8) to the fifth-order of ε , we gain

$$\begin{aligned}
 & \varepsilon^2 a(1 + \lambda t_d) \left\{ b + g\rho_0^2 V'(\rho_c) \right\} \partial_x R \\
 & \varepsilon^3 \left\{ b^2 + \frac{1}{2} a f \rho_0^2 V'(\rho_c) (1 + \lambda t_d) + 4a\gamma\rho_0^2 V'(\rho_0) (1 + \lambda t_d) - \frac{1}{2} a \lambda g \rho_0^2 V'(\rho_c) b t_d^2 - \frac{1}{2} a \lambda b^2 t_d^2 \right\} \partial_x^2 R \\
 & \varepsilon^4 \left\{ \left[\frac{1}{6} a (1 + \lambda t_d) g \rho_0^2 V'(\rho_c) + 4\gamma\rho_0^2 V'(\rho_0) b - 2a\lambda\gamma\rho_0^2 V'(\rho_0) b t_d^2 - \frac{1}{4} a \lambda f \rho_0^2 V'(\rho_c) b t_d^2 + \frac{1}{4} a \lambda g \rho_0^2 V'(\rho_c) b^2 t_d^3 + \frac{1}{4} a \lambda b^3 t_d^3 \right] \partial_x^3 R \right. \\
 & \quad \left. + \frac{1}{6} a (1 + \lambda t_d) g \rho_0^2 V'(\rho_c) \partial_x R^3 + a (1 + \lambda t_d) \partial_T R \right\} \\
 & \varepsilon^5 \left\{ \left[\frac{1}{24} a (1 + \lambda t_d) f \rho_0^2 V'(\rho_c) + \frac{4}{3} a (1 + \lambda t_d) \gamma \rho_0^2 V'(\rho_0) - \frac{1}{12} a \lambda g \rho_0^2 V'(\rho_c) b t_d^2 + a \lambda b^2 t_d^3 \gamma \rho_0^2 V'(\rho_0) + \frac{1}{8} a \lambda f \rho_0^2 V'(\rho_c) b^2 t_d^3 \right. \right. \\
 & \quad \left. \left. - \frac{1}{12} a \lambda g \rho_0^2 V'(\rho_c) b^3 t_d^4 - \frac{1}{12} a \lambda b^4 t_d^4 \right] \partial_x^4 R + \left[\frac{1}{12} a f (1 + \lambda t_d) \rho_0^2 V'''(\rho_c) - \frac{1}{12} a \lambda g \rho_0^2 V'''(\rho_c) b t_d^2 \right] \partial_x^2 R^3 \right. \\
 & \quad \left. + \left[2b - \frac{1}{2} a \lambda t_d^2 g \rho_0^2 V'(\rho_c) - a \lambda t_d^2 b \right] \partial_T \partial_x R \right\} = 0,
 \end{aligned} \tag{15}$$

$$\varepsilon^4 \left[\partial_T R - g_1 \partial_x^3 R + g_2 \partial_x R^3 \right] + \varepsilon^5 \left[g_3 \partial_x^2 R + g_4 \partial_x^4 R + g_5 \partial_x^2 R^3 \right] = 0 \tag{16}$$

where the first derivative and third derivative of the optimal velocity $V(\rho)$ at the critical point (ρ_c, a_c) are $V'(\rho_c) = dV(\rho)/d\rho|_{\rho=\rho_c}$, $V'''(\rho_c) = d^3V(\rho)/d\rho^3|_{\rho=\rho_c}$. By taking $b = -g\rho_0^2 V'(\rho_c)$ and introducing $a = a_c(1 - \varepsilon^2)$, the second-order term and the third-order term of ε are eliminated. We derived the following equation:

where

$$\begin{aligned}
 g_1 &= \frac{1}{6} g \rho_0^2 V'(\rho_c) + \frac{1}{4} \frac{\lambda f \rho_0^2 V'(\rho_c) b t_d^2}{(1 + \lambda t_d)} + \frac{2\lambda b t_d^2 \gamma \rho_0^2 V'(\rho_0)}{(1 + \lambda t_d)} - \frac{4b\gamma\rho_0^2 V'(\rho_0)}{a(1 + \lambda t_d)}, \\
 g_2 &= \frac{1}{6} g \rho_0^2 V'''(\rho_c), \\
 g_3 &= -\frac{1}{2} f \rho_0^2 V'(\rho_c) - 4\gamma\rho_0^2 V'(\rho_0), \\
 g_4 &= \frac{1}{24} f \rho_0^2 V'(\rho_c) + \frac{4}{3} \gamma \rho_0^2 V'(\rho_0) - \frac{1}{12} \frac{\lambda g \rho_0^2 V'(\rho_c) b t_d^2}{(1 + \lambda t_d)} + \frac{1}{8} \frac{\lambda f \rho_0^2 V'(\rho_c) b^2 t_d^3}{(1 + \lambda t_d)} + \frac{\lambda b^2 t_d^3 \gamma \rho_0^2 V'(\rho_0)}{(1 + \lambda t_d)} \\
 & \quad + \frac{1}{a(1 + \lambda t_d)} \left(2b + \frac{1}{2} a \lambda t_d^2 g \rho_0^2 V'(\rho_c) \right) \left(\frac{\lambda f \rho_0^2 V'(\rho_c) b t_d^2}{4(1 + \lambda t_d)} + \frac{2\lambda b t_d^2 \gamma \rho_0^2 V'(\rho_0)}{(1 + \lambda t_d)} - \frac{1}{6} g \rho_0^2 V'(\rho_c) - \frac{4\gamma\rho_0^2 V'(\rho_0) b}{a(1 + \lambda t_d)} \right), \\
 g_5 &= \frac{1}{12} f \rho_0^2 V'''(\rho_c) - \frac{1}{12} \frac{\lambda g \rho_0^2 V'''(\rho_c) b t_d^2}{(1 + \lambda t_d)} - \left(2b + \frac{1}{2} a \lambda t_d^2 g \rho_0^2 V'(\rho_c) \right) \frac{1}{6} \frac{g \rho_0^2 V'''(\rho_c)}{a(1 + \lambda t_d)}.
 \end{aligned} \tag{17}$$

For obtaining the high-order regularized equation, the transformations are introduced:

$$Tt = \left\{ \frac{1}{6} \rho_0^2 Vt(\rho_c) g - \frac{\lambda b t_d^2}{12(1 + \lambda t_d)} \left(3b t_d \rho_0^2 Vt(\rho_c) g - 3\rho_0^2 Vt(\rho_c) f + 2b^2 t_d \right) \right\} T, \quad (18)$$

$$R = \sqrt{\frac{-\rho_0^2 Vt(\rho_c) g - (\lambda b t_d^2 / 2)(1 + \lambda t_d) \left(3b t_d \rho_0^2 Vt(\rho_c) g - 3\rho_0^2 Vt(\rho_c) f + 2b^2 t_d \right)}{\rho_0^2 V'''(\rho_c) g}} Rt.$$

Consequently, the mKdV equation with $O(\varepsilon)$ term is obtained as follows:

$$\partial_{Tt} Rt - \partial_X^3 Rt + \partial_X R^3 + \varepsilon M[Rt] = 0, \quad (19)$$

where $M[Rt] = (1/g_1) \{ g_3 \partial_X^2 Rt + (g_1 g_5 / g_2) \partial_X^2 R^3 + g_4 \partial_X^4 Rt \}$. The solution of the mKdV equation (19) is given by

$$R'_0(X, Tt) = \sqrt{c} \tanh \left[\sqrt{\frac{c}{2}} (X - cTt) \right], \quad (20)$$

where $R'_0(X, Tt) = Rt(X, Tt) - \varepsilon R'_1(X, Tt)$ and $c = 5g_2 g_3 / (2g_2 g_4 - 3g_1 g_5)$.

Thus, the solution of kink-antikink wave of the mKdV equation is yielded as follows:

$$\rho_{j,m} = \rho_c + \varepsilon \sqrt{\frac{g_1 c}{g_2}} \tanh \left\{ \sqrt{\frac{c}{2}} (X - c g_1 T) \right\}. \quad (21)$$

where $\varepsilon^2 = a_c/a - 1$, and the amplitude A of kink-antikink wave is expressed as follows:

$$A = \sqrt{c \frac{g_1}{g_2} \left(\frac{a_c}{a} - 1 \right)}. \quad (22)$$

The solution of kink-antikink wave indicates the coexisting phase which is composed of the free flow phase (low density) and the congested phase (high density). The density of the free flow phase is $\rho_{j,m} = \rho_c - A$, and the density of the congested phase is $\rho_{j,m} = \rho_c + A$. Thereafter, the coexisting curve can be shown as the dotted curve in Figure 2.

Figure 2 reveals the neutral stability lines with solid lines and the coexisting curves with dotted curves for a fixed value of the ratio C_1 , C_2 , and C , the delay time t_d , the cumulative coefficient λ , and the changing path rate γ . The phase diagram can be divided into three regions: the stable region above the neutral line, the metastable region between the neutral stability line and the coexisting curve, and the unstable region below the neutral line. In the metastable region, if the disturbance strength exceeds its critical amplitude, the disturbance will become larger with the time. The pedestrian flow is in the unsteady state, which causes pedestrian congestion. When the disturbance is less than the critical amplitude, pedestrian flow is still in the steady state. In the stable region, pedestrian flow remains the steady state due to the attenuation of disturbance. On the contrary, the disturbance in the unstable region gradually increases with time and eventually develops into kink-antikink wave.

Figure 2(a) plots that the neutral stability lines obviously reduce with increasing value of the ratio C . It is shown that the distribution of pedestrian density impacts the stability of the pedestrian traffic system, and reasonable distribution of pedestrian density can improve the stability of the traffic system. By comparison of Figures 2(a) and 2(b), the increase of delay time t_d leads to the contraction of the unstable region. It indicates that the delay time t_d can significantly enhance the pedestrian traffic stability. Moreover, the stable region is accordingly expanded with the increase of the changing path frequency γ . It means the increase of the changing path frequency γ has a favorable influence on suppressing pedestrian traffic congestion.

5. Simulation and Analysis

In order to verify the results in the stability analysis and nonlinear analysis, we carry out simulation and comparison with the consequence of the theoretic analysis. The periodic boundary condition is adopted in the process of the numerical simulation. The initial density and the critical density are chosen as $\rho(j, m, 0) = \rho_c = 0.25$ and the sensitivity of driver $a = 1.8$. The four-way traffic on square is divided into $L \times L$ lattice with $L = 100$. The small perturbations are added to a two-dimensional four-way pedestrian traffic: $\rho((L/2), (L/2), 1) = 0.1$ and $\rho(L/2 - 1, L/2 - 1, 1) = 0.3$. The unit time step is equal to the inverse of the sensitivity a .

The evolution pattern of density wave is depicted in Figure 3 at 2000 time steps for $C_1 = C_2 = 0.1$ without delay time t_d . As we can see that the fluctuation of density wave in Figure 3(a) is great without changing path frequency. It is easy to cause congestion and is not conducive to evacuation. In Figures 3(b) and 3(c), the fluctuation of density wave is gradually weakened under the increase of path change frequency γ , it indicates that changing path can improve the stability of the traffic system on certain level, and it is consistent with the stability condition equation (12c). When the ratio C is less than or equal to 0.5, Figures 3(b) and 3(d) exhibit that there is no congestion of pedestrian traffic with the increase of the ratio C , which is consistent with the theoretical analysis of system stability.

Figure 4 shows the spatial distribution of density at 2000 time steps for $C_1 = C_2 = C = 0.1$. It is clearly observed that the cumulative effect of delay time t_d can significantly improve the pedestrian traffic stability and eliminate jams of

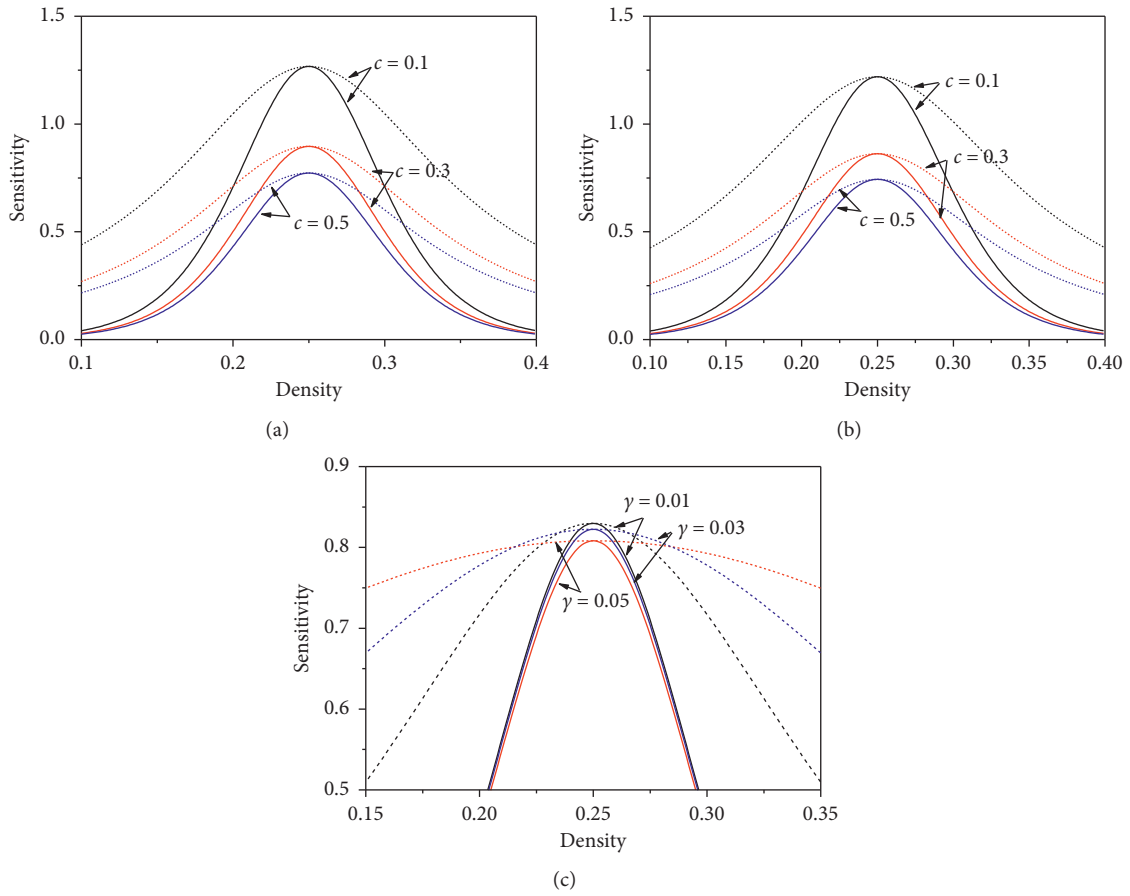


FIGURE 2: Phase diagrams in the (ρ, a) plane for $C_1 = C_2 = 0.1$. The solid curve and dotted curve denote the neutral stability lines and the coexisting curve, respectively. (a) $\lambda = 0.1$, $t_d = 0.1$, and $\gamma = 0.001$. (b) $\lambda = 0.1$, $t_d = 0.5$, and $\gamma = 0.001$. (c) $\lambda = 0.3$, $t_d = 0.3$, and $C = 0.3$.

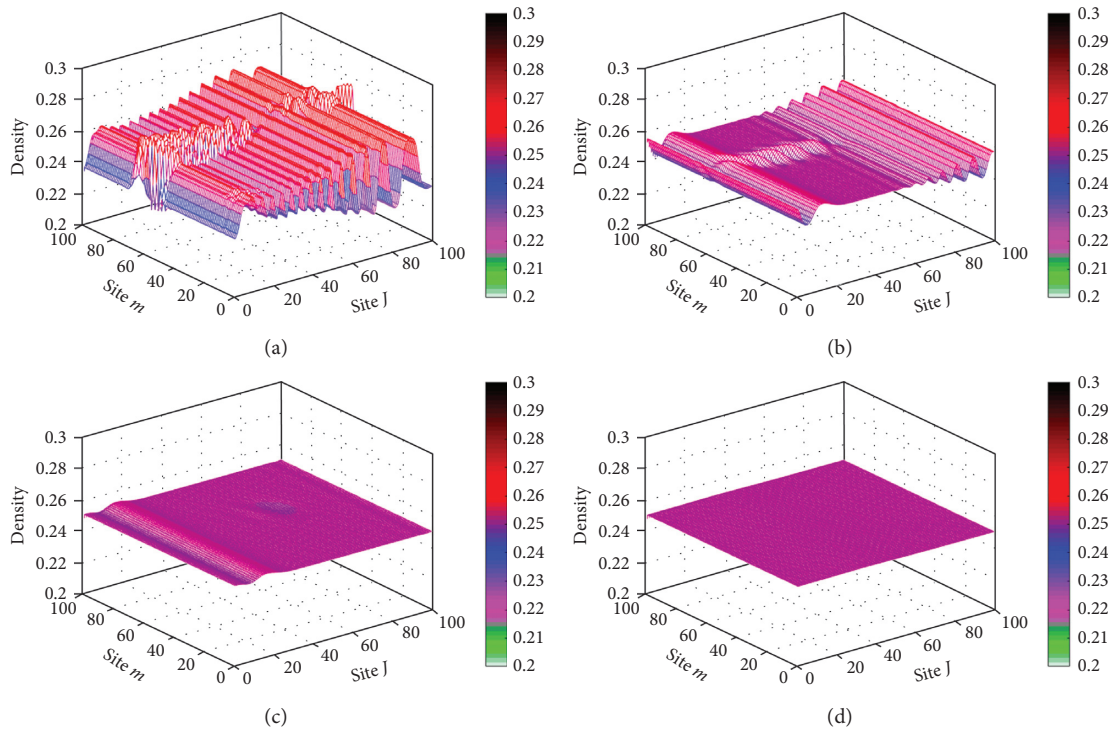


FIGURE 3: The plot of density ρ against space (j, m) for $t = 2000$, $C_1 = C_2 = 0.1$, and $t_d = 0$. (a) $\gamma = 0.0$ and $C = 0.1$. (b) $\gamma = 0.005$ and $C = 0.1$. (c) $\gamma = 0.01$ and $C = 0.1$. (d) $\gamma = 0.005$ and $C = 0.3$.

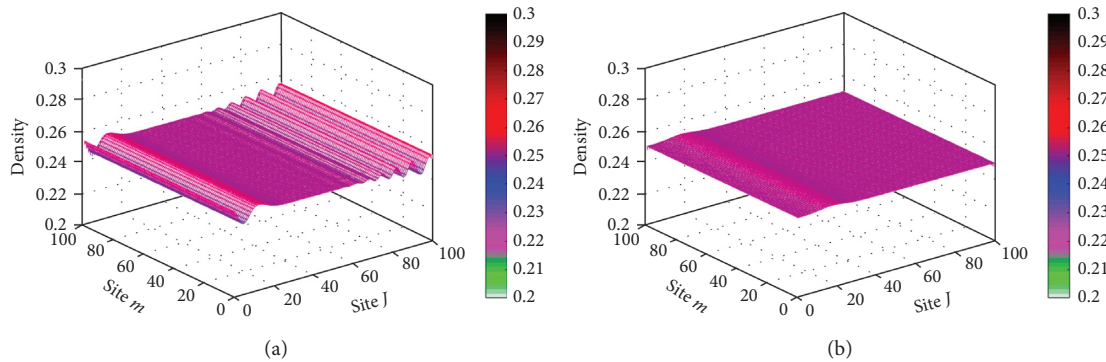


FIGURE 4: The plot of density ρ vs. position (j, m) for $C_1 = C_2 = C = 0.1$ and $t_d = 0.5$. (a) $\lambda = 0.1$ and $\gamma = 0.0$. (b) $\lambda = 0.3$ and $\gamma = 0.0$.

pedestrian traffic from the fluctuation of density wave in Figures 3 and 4. If pedestrians do not think about changing path ($\gamma = 0$), Figure 4(a) shows the great changes in crowd density. When the cumulative effect of delay time t_d enhances, the density change in Figure 4(b) is very small. It indicates the more impact of the greater strength coefficient λ on suppression of traffic congestion. The cumulative term of delay time in equation (5) is suitable to use as a feedback control one.

6. Conclusions

In this paper, a two-dimensional lattice hydrodynamic model of pedestrian traffic flow is proposed considering path change under the cumulative effect of delay time. Using the linear stability analysis, the neutral stability condition is obtained. By performing the nonlinear analysis, the mKdV equation describing the density wave of pedestrian flow is derived and the coexistence curve is gained. The phase diagram is divided into three regions: stable region, unstable region, and metastable region. The theoretical analysis shows that changing path γ and the cumulative effect of delay time t_d can reduce the value of critical point a_c and significantly improve the stability of pedestrian flow. The unstable region can be shrunken by the increase of path change frequency, which may be conducive to crowd evacuation. Numerical simulations further illustrate the improvement of changing path rate and delay time t_d on pedestrian traffic flow. Moreover, increasing ratio C ($C < 0.5$) of eastbound pedestrians and westbound pedestrians to total pedestrians can also improve the stability of pedestrian traffic flow. It indicates pedestrian density must be properly distributed in order to improve the stability of the traffic system.

Data Availability

The data used to support the findings of this study are included within the article's references.

Conflicts of Interest

The authors declare that they have no conflicts of interest.

Acknowledgments

This project was supported by the National Natural Science Foundation of China (Grant nos. 11962002 and 11672176), the Natural Science Foundation of Guangxi, China (Grant no. 2018GXNSFAA138205), and the Doctoral Research Project of Guangxi University of Finance and Economics (Grant no. BS2019027).

References

- [1] Wang, *Shanghai Stampede Kills 36, Injures 49*, CRI ENGLISH, Beijing, China, 2015, <http://english.cri.cn/12394/2015/01/02/3684s859631.htm>.
- [2] C. Xie, *Death Toll in Saudi Arabia Stampede Rises to 769*, CRI ENGLISH, Beijing, China, 2015, <http://english.cri.cn/12394/2015/09/27/3801s897660.htm>.
- [3] X. Hua, *Stampede at Railway Footbridge in India's Mumbai kills 22*, Xinhua, Beijing, China, 2017, http://www.xinhuanet.com/english/2017-09/30/c_136650510.htm.
- [4] L. F. Henderson, "The statistics of crowd fluids," *Nature*, vol. 229, no. 5284, pp. 381–383, 1971.
- [5] D. Helbing, "A fluid-dynamic model for the behavior of pedestrians," *Complex System*, vol. 6, p. 391, 1992.
- [6] R. L. Hughes, "A continuum theory for the flow of pedestrians," *Transportation Research, Part B (Methodological)*, vol. 36, no. 6, pp. 0–535, 2002.
- [7] W. F. Fang, L. Z. Yang, and W. C. Fan, "Simulation of bidirectional pedestrian movement using a cellular automata model," *Physica A: Statistical Mechanics and its Applications*, vol. 321, no. 3-4, pp. 633–640, 2003.
- [8] M. Fukui and Y. Ishibashi, "Self-organized phase transitions in cellular automaton models for pedestrians," *Journal of the Physical Society of Japan*, vol. 68, no. 8, pp. 2861–2863, 1999.
- [9] C. Burstedde, K. Klauck, A. Schadschneider et al., "Simulation of pedestrian dynamics using a two-dimensional cellular automaton," *Physica A: Statistical Mechanics and its Applications*, vol. 295, no. 3-4, pp. 507–525, 2001.
- [10] A. Kirchner, K. Nishinari, and A. Schadschneider, "Friction effects and clogging in a cellular automaton model for pedestrian dynamics," *Physical Review E*, vol. 67, no. 5, Article ID 056122, 2003.
- [11] A. Schadschneider, "Cellular automaton approach to pedestrian dynamics—theory," in *Pedestrian & Evacuation Dynamics*, pp. 75–86, Springer, Berlin, Germany, 2001.
- [12] X. Zheng, W. Li, and C. Guan, "Simulation of evacuation processes in a square with a partition wall using a cellular

- automaton model for pedestrian dynamics,” *Physica A: Statistical Mechanics and Its Applications*, vol. 389, no. 11, pp. 2177–2188, 2010.
- [13] W. G. Weng, T. Chen, H. Y. Yuan et al., “Cellular automaton simulation of pedestrian counter flow with different walk velocities,” *Physical Review E*, vol. 74, no. 3, Article ID 036102, 2006.
- [14] D. Helbing and P. Molnár, “Social force model for pedestrian dynamics,” *Physical Review E*, vol. 51, no. 5, pp. 4282–4286, 1998.
- [15] D. Helbing, I. J. Farkas, P. Molnar, and T. Vicsek, *Simulation of Pedestrian Crowds in Normal and Evacuation Situation Pedestrian and Evacuation Dynamics*, pp. 21–58, Springer, Berlin, Germany, 2002.
- [16] M. H. Afzal, V. Renaudin, and G. Lachapelle, “Magnetic field based heading estimation for pedestrian navigation environments,” in *Procngs of the International Conference on Indoor Positioning & Indoor Navigediation*, IEEE, Guimarães, Portugal, September 2011.
- [17] D. Hartmann, “Adaptive pedestrian dynamics based on geodesics,” *New Journal of Physics*, vol. 12, no. 4, Article ID 043032, 2010.
- [18] R. Jiang and Q.-S. Wu, “Pedestrian behaviors in a lattice gas model with large maximum velocity,” *Physica A: Statistical Mechanics and Its Applications*, vol. 373, pp. 683–693, 2007.
- [19] S. P. Hoogendoorn and P. H. L. Bovy, “Pedestrian travel behavior modeling,” *Networks and Spatial Economics*, vol. 5, no. 2, pp. 193–216, 2005.
- [20] H. Kuang, X. Li, T. S. ong et al., “Analysis of pedestrian dynamics in counter flow via an extended lattice gas model,” *Physical Review E*, vol. 78, no. 6, Article ID 066117, 2008.
- [21] D. Helbing and P. Molnar, “Self-organization phenomena in pedestrian crowds,” *Understanding Complex Systems*, Springer, Berlin, Germany, pp. 569–577, 1998.
- [22] R.-Y. Guo and H.-J. Huang, “A modified floor field cellular automata model for pedestrian evacuation simulation,” *Journal of Physics A: Mathematical and Theoretical*, vol. 41, no. 38, Article ID 385104, 2008.
- [23] H. Yue, H. Guan, J. Zhang, and C. Shao, “Study on bi-direction pedestrian flow using cellular automata simulation,” *Physica A: Statistical Mechanics and Its Applications*, vol. 389, no. 3, pp. 527–539, 2010.
- [24] Y. Zheng, B. Jia, X. G. Li et al., “Evacuation dynamics with fire spreading based on cellular automaton,” *Physica A: Statistical Mechanics and Its Applications*, vol. 390, no. 18-19, pp. 3147–3156, 2011.
- [25] A. Kirchner, K. Hubert, K. Nishinari et al., “Simulation of competitive egress behavior: comparison with aircraft evacuation data,” *Physica A: Statistical Mechanics and Its Applications*, vol. 324, no. 3-4, pp. 689–697, 2003.
- [26] C.-K. Chen, J. Li, and D. Zhang, “Study on evacuation behaviors at a T-shaped intersection by a force-driving cellular automata model,” *Physica A: Statistical Mechanics and Its Applications*, vol. 391, no. 7, pp. 2408–2420, 2012.
- [27] A. Varas, M. D. Cornejo, D. Mainemer et al., “Cellular automaton model for evacuation process with obstacles,” *Physica A: Statistical Mechanics and Its Applications*, vol. 382, no. 2, pp. 631–642, 2007.
- [28] T. Nagatani, “Modified KdV equation for jamming transition in the continuum models of traffic,” *Physica A-Statistical Mechanics & Its Applications*, vol. 261, no. 3-4, pp. 599–607, 1998.
- [29] T. Nagatani, “Jamming transitions and the modified Korteweg-de Vries equation in a two-lane traffic flow,” *Physica A-Statistical Mechanics & Its Applications*, vol. 265, no. 1-2, pp. 297–310, 1999.
- [30] H.-h. Tian, H.-d. He, Y.-f. Wei, X. Yu, and W.-z. Lu, “Lattice hydrodynamic model with bidirectional pedestrian flow,” *Physica A: Statistical Mechanics and Its Applications*, vol. 388, no. 14, pp. 2895–2902, 2009.
- [31] Y. Xue, H.-H. Tian, H.-D. He, W.-Z. Lu, and Y.-F. Wei, “Exploring jamming transitions and density waves in bidirectional pedestrian traffic,” *The European Physical Journal B*, vol. 69, no. 2, pp. 289–295, 2009.
- [32] H. Kuang, T. Chen, X.-L. Li, and S.-M. Lo, “A new lattice hydrodynamic model for bidirectional pedestrian flow considering the visual field effect,” *Nonlinear Dynamics*, vol. 78, no. 3, pp. 1709–1716, 2014.
- [33] J. Zhou, Z.-K. Shi, and Z.-S. Liu, “A novel lattice hydrodynamic model for bidirectional pedestrian flow with the consideration of pedestrian’s memory effect,” *Nonlinear Dynamics*, vol. 83, no. 4, pp. 2019–2033, 2016.
- [34] X. Li, H. Kuang, and Y. Fan, “Lattice hydrodynamic model of pedestrian flow considering the asymmetric effect,” *Communications in Nonlinear Science and Numerical Simulation*, vol. 17, no. 3, pp. 1258–1263, 2012.
- [35] H. M. Yu, R. J. Cheng, and H. X. Ge, “General solution of the modified Korteweg-de-Vries equation in the lattice hydrodynamic model,” *Chinese Physics B*, vol. 19, no. 10, Article ID 100512, 2010.
- [36] P. Redhu and A. K. Gupta, “Delayed-feedback control in a Lattice hydrodynamic model,” *Communications in Nonlinear Science and Numerical Simulation*, vol. 27, no. 1–3, pp. 263–270, 2015.
- [37] P. Redhu and A. K. Gupta, “Effect of forward looking sites on a multi-phase lattice hydrodynamic model,” *Physica A: Statistical Mechanics and Its Applications*, vol. 445, pp. 150–160, 2016.
- [38] G. H. Peng, X. H. Cai, B. F. Cao et al., “Non-lane-based lattice hydrodynamic model of traffic flow considering the lateral effects of the lane width,” *Physics Letters A*, vol. 375, no. 30-31, pp. 2823–2827, 2011.
- [39] T. Wang, Z. Gao, and J. Zhang, “Stabilization effect of multiple density difference in the lattice hydrodynamic model,” *Nonlinear Dynamics*, vol. 73, no. 4, pp. 2197–2205, 2013.
- [40] B.-L. Cen, Y. Xue, X. Wang, D. Chen, and H.-D. He, “A lattice hydrodynamic model of bidirectional pedestrian traffic considering the cumulative effect of delay time,” *IEEE Access*, vol. 7, pp. 168710–168719, 2019.